Journal of Fiber Bioengineering and Informatics 16:4 (2023) 327–339

Cite as: S. Jiang et al.
doi:10.3993/jfbim02961

Numerical Investigation on Convective Heat Transfer of Infants and Adults under Ventilation ⋆

Shu Jiang [a], Jun Li [a,b,*]

[a] *College of Fashion and Design, Donghua University, West Yan'an Road, Shanghai 200051, China*

[b] *Key Laboratory of Clothing Design and Technology, Donghua University, Ministry of Education, West Yan'an Road, Shanghai 200051, China*

Abstract

There is a severe lack of research on the heat transfer mechanisms for various populations, with most studies primarily concentrating on adults. This study aimed to investigate the difference in the convective heat transfer coefficient (h_c) of the whole and individual body parts between infant and adult under ventilation. A numerical model for heat transfer between the human body and the environment was developed and validated against experiments involving a baby thermal manikin. The temperature and airflow fields surrounding the human body and the value of h_c were simulated under seven air velocities ranging from 0.1 m/s to 2.5 m/s. The results indicated that, under natural ventilation, the overall h_c for infants and adults was 4.82 W/m^2·K and 4.29 W/m^2·K, respectively. Infants exhibited higher regional h_c values at their surface than adults, especially on their hands and feet. This discrepancy was more pronounced as the air velocity increased. Furthermore, regression equations were developed for the two body sizes to establish the connection between h_c and air velocity. These findings contribute to a better understanding of the complex interplay between body size and convective heat transfer, providing fundamental data for enhancing the accuracy of infant thermal response predictions by incorporating more precise boundary conditions.

Keywords: Convective Heat Transfer Coefficient; Numerical Simulation; Body Size; Infant; Air Velocity

1 Introduction

The convective heat transfer coefficient (h_c) at the surface of the human body plays a critical role in determining the heat transfer between the human body and the environment. It is also an essential input parameter in human thermal regulation models to predict thermal responses

⋆Project financial support from the Fundamental Research Funds for the Central Universities (Grant No. 2232023G-08), International Cooperation Fund of Science and Technology Commission of Shanghai Municipality (Grant No. 21130750100) and Graduate Student Innovation Fund of Donghua University (Grant No. CUSF-DH-D-2022048).

*Corresponding author.
Email address: lijun@dhu.edu.cn (Jun Li).

1940–8676 / Copyright © 2023 Textile Bioengineering and Informatics Society
Dec. 2023

or comfort [1]. To date, many manikin tests and numerical studies have been performed to measure the value of this coefficient under diverse conditions. However, most research in this area has focused on male or female adult body shapes, while populations with other body sizes have received little research attention.

Infants, characterised by their distinctively smaller body size and shorter length than adults, exhibit unique thermal characteristics. The smaller characteristic length theoretically leads to a lower Rayleigh number (Ra) and a higher h_c under natural convection. As a result, infants are more susceptible to thermal environments and experience faster heat loss at low temperatures than adults. To accurately measure the value of h_c for infants, researchers have developed manikins that mimic the body size of infants, enabling the measurement of h_c under natural convection [2, 3]. Recently, numerical models have been constructed to visualise airflow patterns and temperature distributions inside neonate incubators and simulate convective heat transfer [4-6]. Nevertheless, the coefficients from this research are difficult to compare with the results from adult research due to inconsistent body postures or varied testing conditions.

Fukazawa et al. [7] employed two types of thermal manikins (a female adult shape with a height of about 168 cm and an infant shape aged six months with a height of 65 cm) in an artificial chamber with a uniform environmental condition to compare the difference in the h_c between adult and infant. The results indicated that the overall h_c for the adult manikin was 3.9 $W/m^2 \cdot K$, while that for the infant manikin revealed 6.2 $W/m^2 \cdot K$. For regional body parts, significantly larger h_c values at the head, back trunk and upper limbs were observed for infants. It is important to note that this research was only conducted under natural convection. However, higher air velocity may occur, especially on outdoor occasions, which differs from that commonly encountered indoors. Infants under one-year-old are often exposed to forced convective flow generated by indoor ventilation systems or outdoor air. This presents a potential risk of rapid heat loss for infants in windy conditions. Since infants have poor abilities to regulate body temperature [8], it is necessary to evaluate the convective heat transfer of infants and discern the differences from adults under the effects of wind.

The current study aims to examine and compare the convective heat transfer between infants and adults under natural and forced ventilation, utilising validated Computational Fluid Dynamics (CFD) models. To achieve this, simulations were performed at seven levels of air velocity ranging from 0.1 m/s to 2.5 m/s, covering the typical range of air speed in indoor and outdoor environments. This study provides specific information on the airflow near individual body parts of infants and adults, and the formulas were developed for predicting regional h_c for both populations. These findings contribute to a better understanding of the complicated interplay between body size and convective heat transfer under varied air velocities and provide basic data for predicting human thermal response with more accurate boundary conditions. From a practical standpoint, the specific guidance on thermal protection for infants will be made referring to adult caregivers, especially addressing the vulnerability of certain body parts.

2 Methodology

To investigate and visualise the heat transfer around the human body, the first step of this study was to determine the method of CFD simulation. Infant manikin experiments were conducted in an artificial climate chamber. The airflow and temperature distributions inside the chamber, as well as the heat loss of baby manikin, were predicted using COMSOL Multiphysics 5.6 (COMSOL,

Inc., USA). Comparisons were made between the experiment and simulation results to validate the modelling method. The second step was to perform a parametric study based on the validated CFD models. A numerical manikin in the shape of adults was added to compare the heat transfer between infants and adults. The whole and regional h_c under different levels of air velocity were derived based on simulation results.

2.1 Determination of Simulation Method

2.1.1 Physical Experiments

The experiments were performed in an artificial climate chamber with a dimension of 6.00×5.00×2.44 m^3. A standing baby manikin (Thermetrics, Seattle, WA, USA, height: 73 cm, surface area: 0.44 m^2) was located in the centre of the chamber and lifted 49 cm from the floor by aluminium support (Fig. 1). The manikin consisted of a carbon fibre-epoxy body form with distributed heating wires and wire sensors. The painting of the skin surface had a similar emissivity of 0.95 with the human body. It contained 19 independently heated thermal segments, and all segments were controlled at 34±0.1 °C. The power generated to maintain the surface temperature was considered equivalent to heat loss from the human body. The chamber's air temperature and relative humidity were set to 21 °C and 50%, respectively. The airflow created by the ventilator entered the chamber from two inlets, and the air velocity at the inlet was measured at 1.2 m/s using omnidirectional anemometers (Sensor Electronic, SensoAnemo5100LSF, accuracy: ±0.02 m/s ±1.5%). This value was applied as the inlet boundary condition for the simulations. Fifty-four measurement points at six different heights distributed within a range of 80 cm from the manikin were additionally chosen to validate air velocity between models and simulations. Each point was measured for 5 minutes at 10-second intervals to obtain the average. Besides, the air velocity near the head, abdomen, frontal thigh, up arm and back of the manikin was detected using thermocouples (Omega, 5TC-TT-K-36-72, diameter: 0.13 mm, calibration accuracy: ±0.02 °C). According to the thickness of the microclimate surrounding the human body measured by Voelker et al. [9], seven points were selected within a range of 16 cm from each segment surface. Therefore, thirty-five points were selected for temperature measurement. At the same time, the heat flux at each manikin segment was also recorded during the temperature measurement. Temperatures and heat fluxes were recorded during 20 minutes at 20-second intervals, and the average and standard deviation (SD) were calculated.

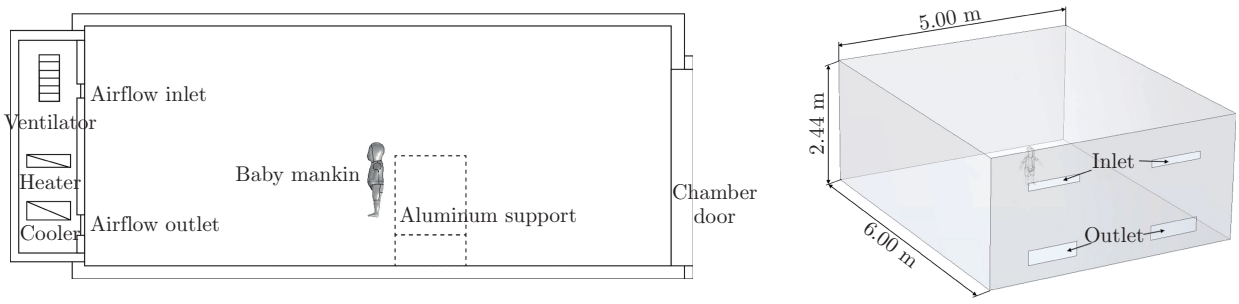


Fig. 1: Diagram of the climate chamber

2.1.2 Geometry Model

Geometry models for chamber and infant manikin were established using COMSOL software. Only half of the models were involved in the simulation to reduce the computational cost. The virtual chamber had a size of 6.00×2.50×2.44 m^3, which was consistent with the size of the half of the artificial climate chamber. It contained one airflow inlet and one outlet on the same wall. A hand-held 3D laser scanner (Handycan700, resolution: 0.050 mm, accuracy: 0.030 mm) was used to capture the 3D data of the baby manikin surface. Geomagic Studio software (Geomagic Inc., USA) was applied to post-process and generate an STP file of a 3D manikin model, which was finally imported into COMSOL software. The location of the virtual baby manikin was the same as the physical experiment.

2.1.3 Governing Equation

The convective heat transfer was simulated by coupling the turbulence flow and heat transfer in fluids in COMSOL software. The airflow distribution around the two manikins was predicted using a low Re k-ε turbulence model. The surface-to-surface (S2S) radiation model was used to compute the radiative heat transfer between the manikin surfaces and the chamber walls.

2.1.4 Mesh Generation

The computational domain was divided into two parts: the semi-cylinder around the virtual manikin and the remaining part of the domain. Unstructured grids are more flexible in mesh distribution and, thus, often used for simulating the airflow around complicated geometries. Therefore, the triangular surface meshes were generated on the manikin surface, and the tetrahedral domain mesh was used to mesh two domains. Five layers of prism mesh with an initial thickness of 0.5 mm and a growth rate 1.2 were created around the manikin surface to make the value of y+ near and even lower than 1. Finally, the mesh number of 0.683 million was chosen for simulation and regarded as mesh-independent.

2.1.5 Model Validation

The simulated and experimental values were used to compare air velocity, temperature, and heat flux. The modelling method has been fully validated, and the detailed process and results were recorded in our previous research [14].

2.2 CFD Simulations under Windy Conditions

2.2.1 Geometry Model and Mesh Generation

A more generic-shaped climate chamber with dimensions of 6.00×2.00×2.40 m^3 was created in COMSOL, with the inlet and outlet facing each other (Fig. 2). The virtual infant and adult manikins were respectively placed in the centre of the chamber, facing the inlet, with their feet 10 cm off the ground. Each virtual manikin was divided into nine body parts, and the specific division of these parts is detailed in Table 1. After mesh independent study, the mesh number generated for the infant and adult models was 0.649 million and 2.575 million, respectively.

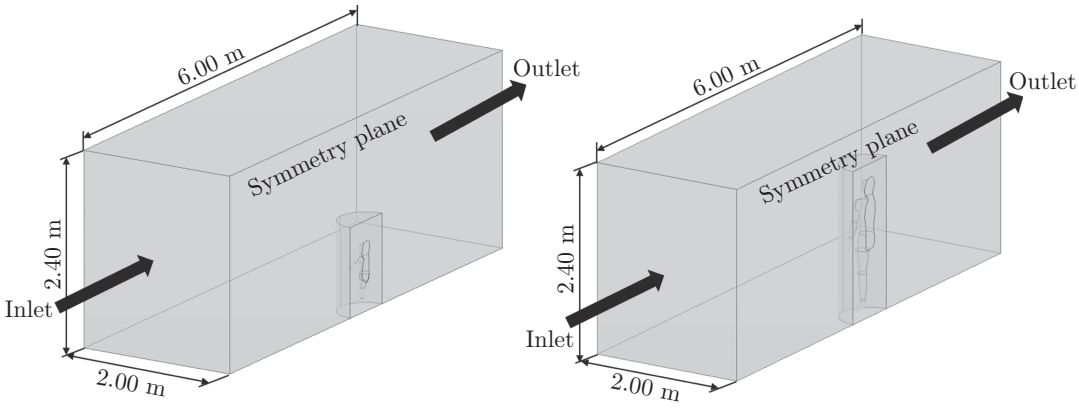


Fig. 2: Geometry models

Table 1: The surface area of body parts (half of the manikin)

Body part	Surface area (m^2)	
	Infant	Adult
Head	0.045	0.071
Chest	0.035	0.099
Back	0.025	0.092
Upper arm	0.015	0.074
Lower arm	0.011	0.026
Hand	0.010	0.036
Upper leg	0.041	0.235
Lower leg	0.022	0.110
Foot	0.015	0.056

2.2.2 Boundary Conditions

Seven distinct windy circumstances with variable input velocities (0.1-2.5 m/s) were developed for each manikin. The effects of air velocity on convective heat transfer between the body surface and the surrounding environment were investigated by comparing h_c, calculated by Eq. (1). Table 2 lists the specific boundary conditions.

$$h_c = \frac{q_c}{t_{sk} - t_a} \tag{1}$$

Where q_c (W/m^2) is the convective heat flux at the manikin surface.

2.2.3 Statistical Analysis

To examine the variation in h_c between newborns and adults, a paired samples t-test was performed. The significance level was established at $p<0.05$ when using the SPSS v24.0 program (IBM, Inc., USA). The regression analysis was performed with the simulated h_c and v_a by MATLAB R2018a software (MathWorks, Inc., USA). Both the overall and individual body parts of

Table 2: Boundary conditions for parametric study

Boundary conditions	
Inlet	Velocity: 0.1, 0.3, 0.5, 1.0, 1.5, 2.0, 2.5 m/s
	Turbulence intensity: 10.0%
	Temperature: 21.0 °C
Outlet	Pressure outlet: static pressure, P=0
Wall	Adiabatic
	Velocity: no slip
Baby manikin	Velocity: no slip
	Temperature: 34 °C
Adult manikin	Velocity: no slip
	Temperature: 34 °C
Air	Weakly compressible

infant and adult manikin were included in the analysis. R^2 was used to rate how well an equation fits the data.

3 Results

3.1 Convective Heat Transfer Coefficient of the Whole Body

The simulated overall h_c for the infant and adult manikins at various airspeeds (v_a) is shown in Fig. 3. The difference in h_c between the two manikins, divided by the h_c for the adult, is used to compute the change in h_c for the infant. The findings showed that the overall h_c for the infant and adult under natural ventilation (i.e., 0.1 m/s v_a) was 4.82 W/m^2·K and 4.29 W/m^2·K, respectively. The h_c for infants was significantly higher than that for adults ($p<0.05$), with a difference ranging from 0.50-0.85 W/m^2·K. The infant's change in h_c dropped quickly, then fell more slowly before stabilising at 2.7%.

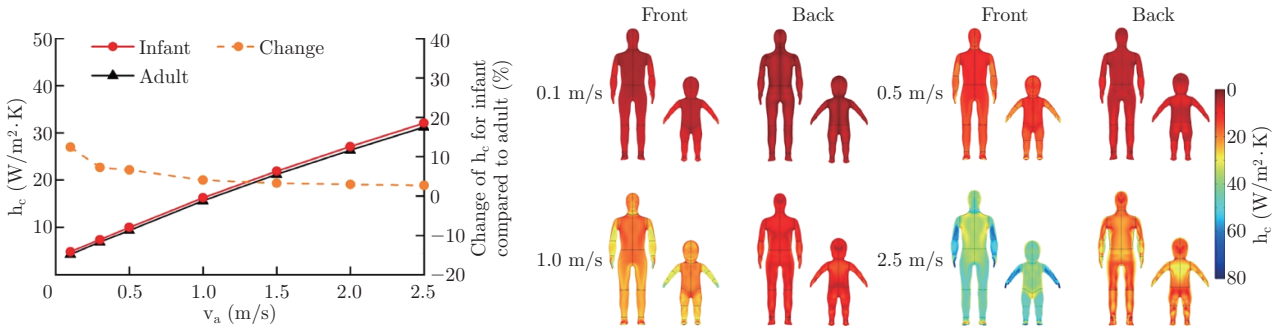


Fig. 3: Overall h_c for the infant and adult manikin

The distributions of h_c for infant and adult at the v_a of 0.1, 0.5, 1.0 and 2.5 m/s were extracted and depicted in Fig. 3. Dark blue denotes higher h_c, while dark red denotes lower h_c. As it

increased, the hue of the human body's front changed from dark red to blue-green, showing a strong effect of the frontal wind on this region. The solid human body blocked the wind, and the back of the body was less affected by it. The h_c distribution differed between infants and adults, and this change was particularly noticeable in the arms and legs.

3.2 Convective Heat Transfer Coefficient of Individual Body Parts

Fig. 4 shows the simulated regional h_c for the infant and adult manikin and the change of h_c for the infant at seven levels of v_a. All the regional h_c values for the infant were significantly greater than those for the adult ($p<0.05$), except at the upper leg ($p = 0.094$), where the infant had lower h_c as v_a exceeded 0.5 m/s. Under increased airflow, the difference in h_c between the two manikins was more obvious, especially at the hand and foot.

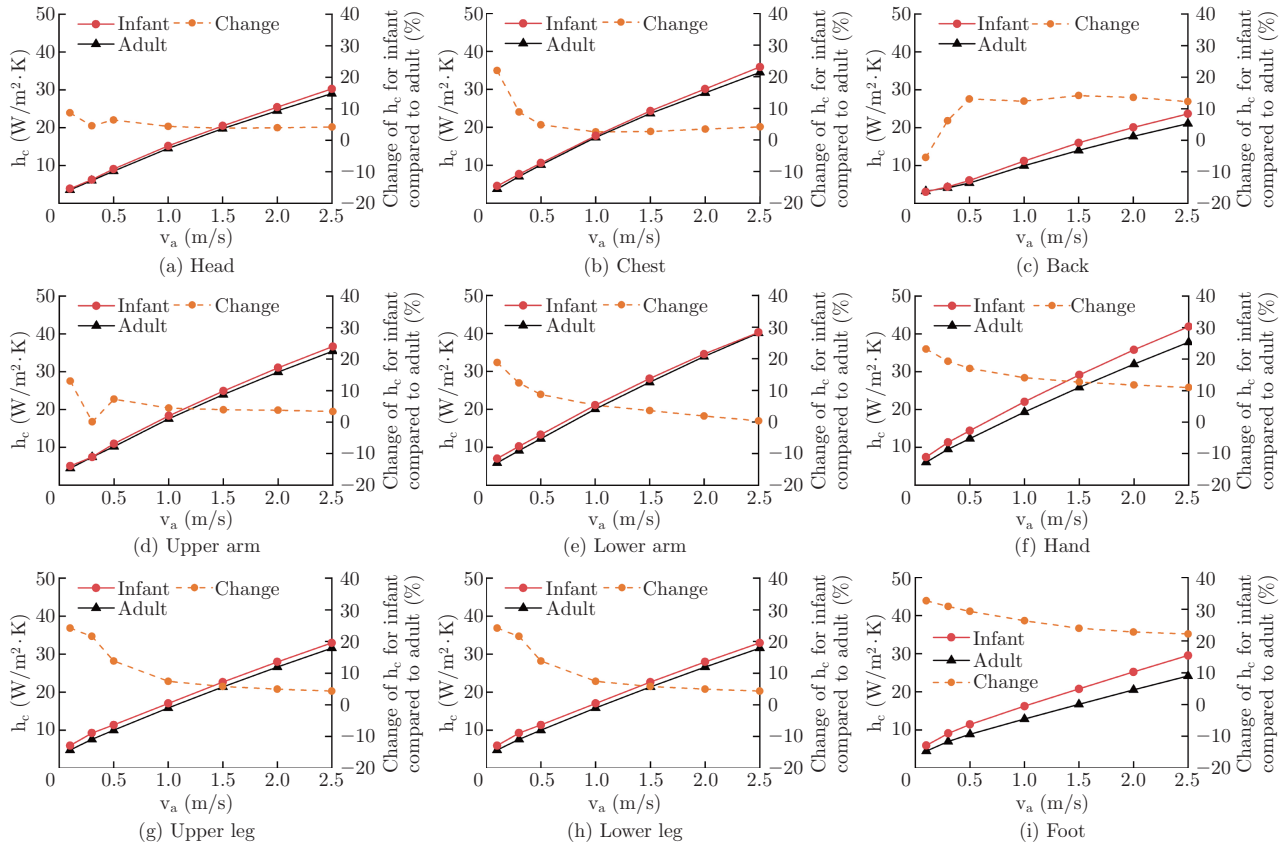


Fig. 4: Regional h_c for the infant and adult manikin

When v_a was less than 0.5 m/s, the infant's change in h_c fluctuated often, but as soon as v_a exceeded 0.5 m/s, it stabilised. In general, when v_a increased, the curve of the change of regional h_c decreased. There is a major exception, though, as the h_c in the back region significantly increases when the v_a increases from 0.1 m/s to 0.5 m/s, from −5.5% to 13.1%. Following that, it stabilises at roughly 13%.

The differences in regional h_c across each body part were also minimal at lower v_a values, with a range of 3.06-7.42 W/m^2·K at 0.1 m/s v_a. These differences grew as v_a rose, leading to a wider range of regional h_c at 2.5 m/s v_a, ranging from 21.07 W/m^2·K to 41.92 W/m^2·K. The highest regional h_c was always observed at the hand, with the lowest at the back.

4 Discussion

4.1 Difference in the Overall h_c between Infant and Adult

The overall h_c of the infant was significantly higher than the adult, as illustrated visually in Fig. 3. This result is consistent with Fukazawa et al.'s study [7], in which a physical experiment produced a comparable result that was attributed to the discrepancy in Rayleigh numbers (Ra) brought on by height variations between the two populations. In this study, the distribution of temperature and airflow around the human body was further observed (Figs. 5 and 6), and it was found that the length of body parts significantly influenced the formation of thermal plumes. Natural convection predominated at 0.1 m/s v_a, and buoyancy was the main force behind the airflow. A warm thermal plume encircled both the adult and the infant, resulting in a low overall h_c. The adult's longer torso served as a strong barrier, deflecting the wind blowing in its direction and causing a fully grown thermal plume to travel straight up behind its back. Nevertheless, the infant's torso length was too short to allow the thermal plume to develop fully in the height direction, and the undeveloped thermal plume was further impaired by the frontal wind, enhancing convective heat transfer between the infant and its surroundings. The thermal plume surrounding the human body changed greatly as v_a reached 0.5 m/s. The airspeed behind the human body was significantly lower than the remaining regions, forming a thermal plume at the back. Due to the longer torso, more heat builds up around the adult than the infant, lowering h_c for the adult. Similar outcomes were seen when forced convection occurred at 2.5 m/s.

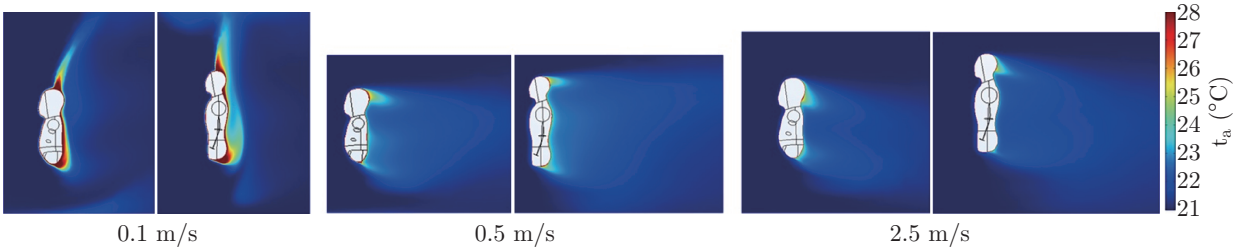


Fig. 5: Simulated temperature distribution at infant and adult sagittal plane under three air velocities

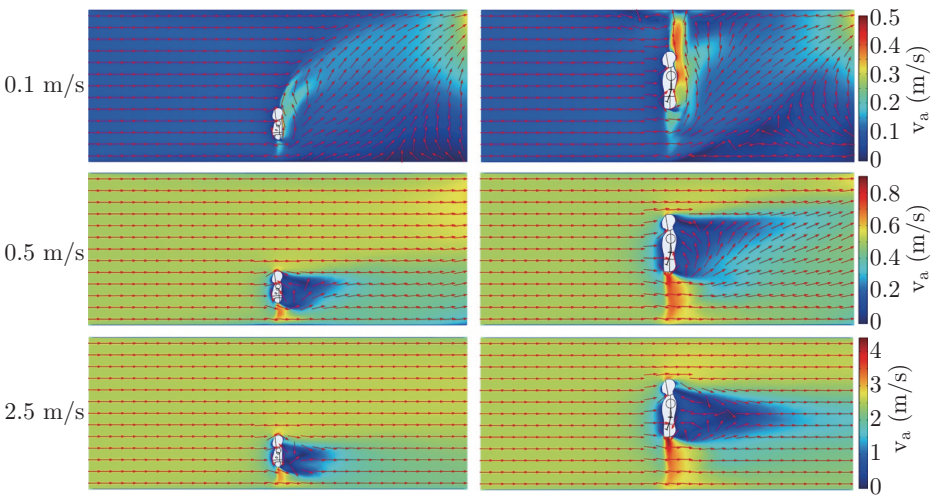


Fig. 6: Simulated airflow at infant and adult sagittal plane under three air velocities

A larger surface area-to-mass ratio also has an impact on heat dissipation. Assuming that the body densities of infants and adults are similar, the surface area-to-mass ratio can be converted by surface area-to-volume. The infant manikin's surface area-to-volume was 36.5, which is about 1.4 times adults, further leading to a larger overall h_c at the infant surface.

4.2 Difference in the Regional h_c between Infant and Adult

Fig. 4 illustrates that the h_c at the limbs and chest were noticeably greater than that at the head and back, both for the infant and adult, which was consistent with the observations of previous studies [9, 11, 15]. This phenomenon was attributed to the effective projected area of body parts with respect to the wind.

Compared to the adult, the infant exhibited a significantly higher regional h_c, especially at the hand and foot, where the changes of regional h_c for the infant were always more than 10%. To better understand the difference in regional h_c between adults and infants, the v_a distribution around the hand and the foot was extracted and displayed in Fig. 7. The results showed that the v_a around the hand and foot showed extreme heterogeneity in the transverse and longitudinal sections. Higher v_a was observed on the two sides, parallel to the wind direction, compared with the windward and leeward sides. Interestingly, the air velocity around the infant's feet seemed slightly lower than the adult's, contradicting the higher regional h_c result. This study speculated that the difference in the h_c between infants and adults in these regions may be related to the intensity of the turbulence. Due to the smaller scale of the body parts, the infant may have higher Reynolds numbers (Re), resulting in greater turbulence intensity (Eq. (2) and Eq. (3)). Previously, some scholars reported that the higher turbulence intensity enlarges the h_c of body

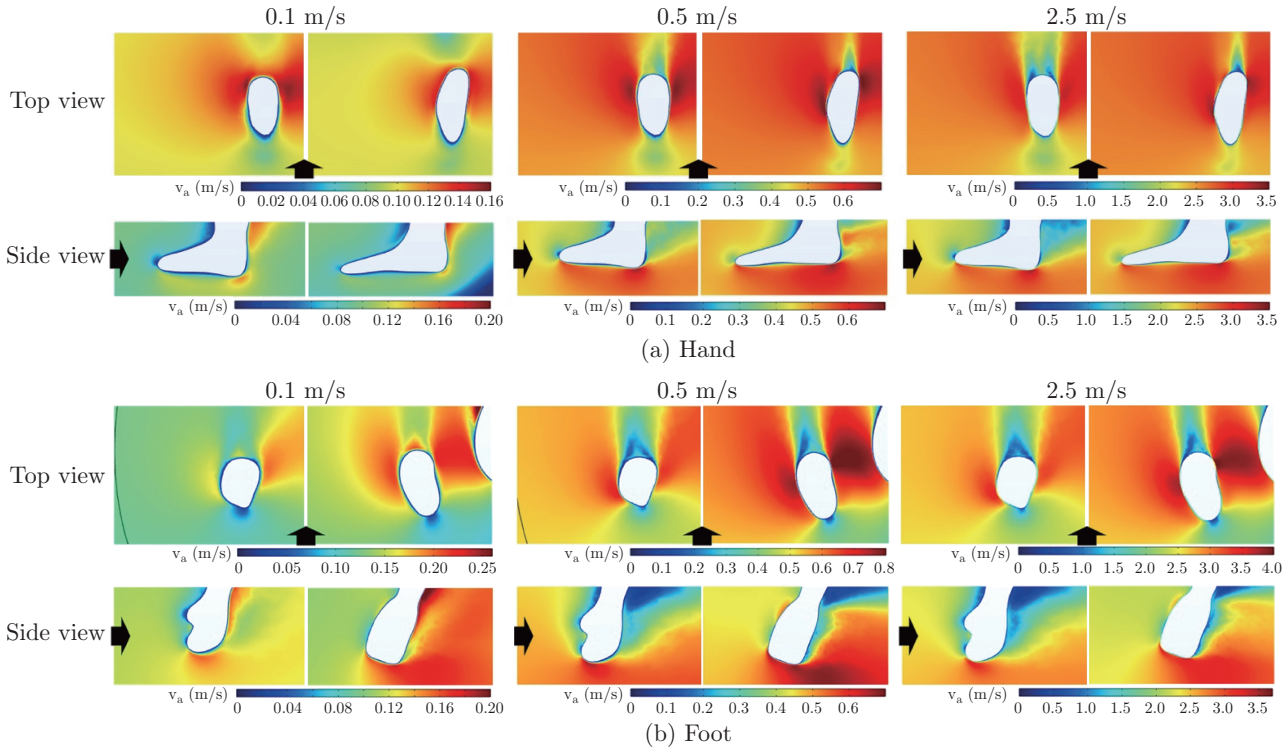


Fig. 7: Simulated v_a distribution around the hand and foot of infant and adult

parts, and the influence of turbulence intensity became more pronounced at high air speed [16]. As a result, most body parts of infants were prone to cooling down more quickly than adults, with the hands and feet being the most vulnerable to heat loss. Given that infants have fully undeveloped thermoregulation, providing adequate thermal protection for infants is vital, especially for their extremities.

$$\mathrm{Re} = \frac{u \times L}{\nu} \tag{2}$$

$$\mathrm{TI} = 0.16\mathrm{Re}^{-\frac{1}{8}} \tag{3}$$

Where Re (dimensionless) is the Reynolds number, u (m/s) is the velocity of airflow, L (m) is the characteristic length of body parts, ν (m^2/s) is the kinematic viscosity of air, and TI (%) is the turbulence intensity of air.

A special case in which the adult's height was higher in the upper legs than in infants was observed, possibly due to the difference in segment division. Moreover, it was found that the discrepancies in regional h_c between the infant and adult varied among different body regions, which may be correlated with many factors, such as the height position of body segments, the buoyancy of the air, and the positional relationships between body segments. Therefore, it demonstrated the significance of obtaining the airflow condition near body parts to comprehensively understand convective heat transfer [17].

4.3 Regression Equations of h_c on v_a

To explain the effect of v_a, the Richardson number (Ri) was calculated by Eq. (4) to determine the nature of the flow around the manikins (Table 3). When $v_a = 0.1$ m/s, the Ri number was above 16, indicating that the airflow was dominated by natural convection. When $0.3 \leqslant v_a \leqslant 1.5$ m/s, it turned to mixed convection, where natural and forced convection acted together to enhance the heat transfer. When $v_a > 1.5$m/s, forced convection predominated.

Table 3: Richardson number (Ri) under different ventilation conditions

Air velocity (m/s)	0.1	0.3	0.5	1	1.5	2	2.5
Adult	75	8.3	3	0.75	0.33	0.19	0.12
Infant	31	3.4	1.24	0.31	0.14	0.08	0.15
Nature of flow	Natural	Mixed	Mixed	Mixed	Mixed/Forced	Forced	Forced

Eq. (5), which was often adopted for the prediction of h_c, was employed in this study. The coefficients and corresponding R^2 are respectively exhibited in Table 4. Figure 8 shows the derived regression equations of the overall h_c in this study and those in previous studies [9, 10, 12, 15, 16]. It showed that the predicted h_c for the adult in this paper was slightly lower than that reported in Ichihara et al.'s study [10] when v_a was less than 1.0 m/s but slightly higher when v_a exceeded 1.0 m/s. Generally, it revealed slightly higher h_c values than most previous studies, especially under forced ventilation.

$$\mathrm{Ri} = \frac{\mathrm{Gr}}{\mathrm{Re}^2} \tag{4}$$

$$h_c = b \cdot v_a^n \tag{5}$$

Table 4: Coefficients for regression equations of h_c

Body segment	Infant			Adult		
	b	n	R^2	b	n	R^2
Whole body	16.32	0.7733	0.9998	15.64	0.752	1
Head	15.14	0.7524	0.9999	14.48	0.7592	1
Chest	17.8	0.763	0.9999	17.27	0.7558	0.9998
Back	11.22	0.8258	0.9987	9.888	0.832	0.9995
Upper arm	18.37	0.7542	1	17.51	0.7713	1
Lower arm	21.26	0.6965	0.9998	20.16	0.7486	0.9997
Hand	22.33	0.6812	0.9991	19.54	0.7137	0.9993
Upper leg	15.15	0.7318	0.9998	15.82	0.7562	1
Lower leg	17.4	0.6876	0.9977	16.05	0.7332	0.9992
Foot	16.55	0.6158	0.9953	13.11	0.6531	0.9962

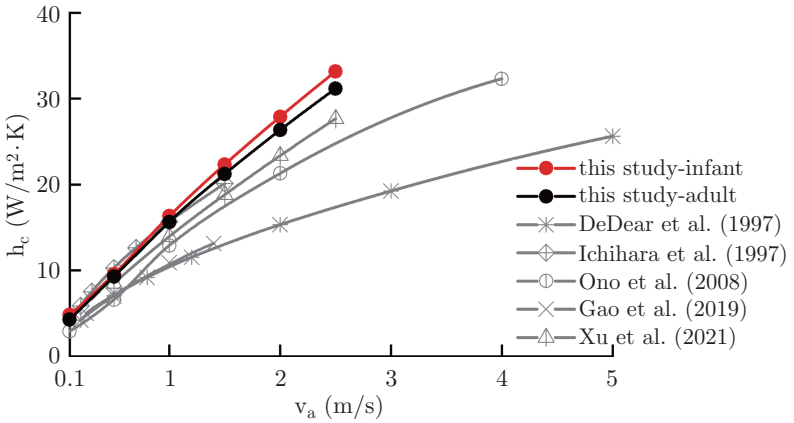


Fig. 8: Comparison of regression equations for the overall h_c in this study and those in previous studies

Previously, many scholars have established relevant models and obtained some conclusions regarding the variation of h_c with airspeed. The predicted h_c by the regression equation developed in this study was close to that developed by Ichihara et al. [10]. Compared with these results in previous studies, the overall h_c derived in this study was slightly higher, which can be explained by the diversity in boundary conditions (e.g., inlet temperature, turbulence intensity) and geometry of climate chamber and manikin. For example, the inlet temperature was in a range of 22-30 °C in the remaining four studies, which reduced the temperature gradient between the human body surface and environment, resulting in less convective heat transfer. Generally, this paper's variation trend of h_c agreed with that in other research, reflecting the derived model's effectiveness.

Due to ethical issues, few researchers have discussed heat transfer in infants. Only a few studies reported the temperature and airflow conditions in an incubator for the thermal care of preterm newborns, and most of them focused on the impacts of air temperature on the convective and radiative heat transfer coefficient of infants [18, 19]. However, as infants older than one week are typically exposed to the same environment as adult caregivers, including ventilation in outdoor or indoor settings, there is a need to further investigate convective heat transfer around infants in

such conditions. This study proposed the regression equation of h_c for the infant under common air velocities, and the corresponding curve was higher than previous studies focused on adults. The outcomes of this study will help evaluate the convective heat transfer around infants under more conditions and predict thermal comfort based on the thermal sensations of adult caregivers. It can also provide a valuable basis for formulating strategies to safeguard infants from thermal discomfort and potential risks associated with convective heat transfer.

5 Conclusion

In this study, the h_c of whole and individual body parts for infants and adults under seven levels of air velocity were investigated and compared using validated CFD numerical models. Compared to the previous studies, there are new contributions, as follows:

(1) The overall h_c for infants and adults under natural ventilation was 4.82 $W/m^2 \cdot K$ and 4.29 $W/m^2 \cdot K$, respectively. Infants always have a pronouncedly higher overall h_c than adults, ranging from 0.50 $W/m^2 \cdot K$ to 0.85 $W/m^2 \cdot K$. This may be related to the development of thermal plumes affected by the length of body parts.

(2) The higher h_c of individual body parts was observed for infants, compared with adults, especially at the hands and feet. This discrepancy was widened as the increment of v_a. An extra light underwear or cover may be necessary for infants compared to adults. More thermal protection for infants' hands and feet, such as mittens and socks, is recommended.

(3) Regression equations of h_c for infants and adults were established, which will help improve the thermal comfort prediction for infants.

Besides, some limitations should be acknowledged. Radiative heat transfer was not included in this research. However, radiative heat flux is a dominating factor in heat transfer, especially at low air velocities. In the future, it is vital to examine the radiative and convective heat transfer for different populations under various environmental conditions, such as air and radiative temperatures.

Acknowledgement

The authors would like to acknowledge the financial support from the Fundamental Research Funds for the Central Universities (Grant No. 2232023G-08), International Cooperation Fund of Science and Technology Commission of Shanghai Municipality (Grant No. 21130750100) and Graduate Student Innovation Fund of Donghua University (Grant No. CUSF-DH-D-2022048).

References

[1] Yang J, Zhang S. Three-dimensional simulation of the convective heat transfer coefficient of the human body under various air velocities and human body angles. Int J Therm Sci [Internet]. 2023;187 (November 2022): 108171. Available from: https://doi.org/10.1016/j.ijthermalsci.2023.108171

[2] Ostrowski Z, Rojczyk M. Natural convection heat transfer coefficient for newborn baby: Thermal manikin assessed convective heat loss. Heat Mass Transf. 2018; 54(8): 2395-2403.

[3] Sarman I, Bolin D, Holmér I, Tunell R. Assessment of thermal conditions in neonatal care: Use of a manikin of premature baby size. Am J Perinatol. 1992; 9(4): 239-246.

[4] Yamaguchi T, Hanai S, Horio H, Hasegawa T. An application of computational fluid mechanics to the airflow in an infant incubator. Ann Biomed Eng. 1992; 20(5): 497-503.

[5] Wrobel L C, Ginalski M K, Nowak A J, Ingham D B, Fic A M. An overview of recent applications of computational modelling in neonatology. Philos Trans R Soc A Math Phys Eng Sci. 2010; 368(1920): 2817-2834.

[6] Hannouch A, Habchi C, Lemenand T, Khoury K. Numerical evaluation of the convective and radiative heat transfer coefficients for preterm neonate body segments inside an incubator. Build Environ. 2020; 183: 107085.

[7] Fukazawa T, Ando T, Ikeda S, Yamaguchi A, Holmér I, Tochihara Y. Convective heat transfer coefficient from baby is larger than that from adult. In: The 13th International Conference on Environmental Ergonomics. 2009: 318-322.

[8] Kurazumi Y, Sakoi T, Yamashita K, Fukagawa K, Kondo E. Thermal manikin of infant. Engineering. 2019; 11: 735-754.

[9] Voelker C, Alsaad H. Simulating the human body's microclimate using automatic coupling of CFD and an advanced thermoregulation model. Indoor Air. 2018; 28(3): 415-425.

[10] Jiang S, Li J. 3D Numerical Investigation of Heat Transfer of Infants in the Indoor Environment. AATCC J Res. 2022; (1882): 247234442211366.

[11] De Dear R J, Arens E, Hui Z, Oguro M. Convective and radiative heat transfer coefficients for individual human body segments. Int J Biometeorol. 1997; 40(3): 141-156.

[12] Xu J, Psikuta A, Li J, Annaheim S, Rossi R M. A numerical investigation of the influence of wind on convective heat transfer from the human body in a ventilated room. Build Environ. 2021; 188: 107427.

[13] Kuwabara K, Mochida T, Nagano K, Shimakura K. Experiments to determine the convective heat transfer coefficient of a thermal manikin. Environ Ergon. 2005; 3(C):423-429.

[14] Ono T, Murakami S, Ooka R, Omori T. Numerical and experimental study on convective heat transfer of the human body in the outdoor environment. J Wind Eng Ind Aerodyn. 2008; 96(10-11): 1719-1732.

[15] Croitoru C, Nastase I, Bode F, Sandu M. Assessment of virtual thermal manikins for thermal comfort numerical studies. Verification and validation. In: E3S Web of Conferences. EDP sciences; 2019: 1-7.

[16] Gao S, Ooka R, Oh W. Formulation of human body heat transfer coefficient under various ambient temperature, air speed and direction based on experiments and CFD. Build Environ [Internet]. 2019; 160: 106168. Available from: https://doi.org/10.1016/j.buildenv.2019.106168

[17] Ichihara M, Saitou M, Nishimura M, Tanabe S. Measurement of Convective and Radiative Heat Transfer Coefficients of Standing and Sitting Human Body By Using a Thermal Manikin. J Archit Plan (Transactions AIJ). 1997; 62(501): 45-51.

[18] Elabbassi E B, Chardon K, Bach V, Telliez F, Delanaud S, Libert J P. Head insulation and heat loss in naked and clothed newborns using a thermal mannequin. Med Phys. 2002; 29(6): 1090-1096.

[19] Fic A M, Ingham D B, Ginalski M K, Nowak A J, Wrobel L C. Modelling and optimisation of the operation of a radiant warmer. Med Eng Phys [Internet]. 2014; 36(1): 81-87. Available from: http://dx.doi.org/10.1016/j.medengphy.2013.10.003